

NOAA Technical Memorandum NWS WR-151

NMC MODEL PERFORMANCE IN THE NORTHEAST PACIFIC

James E. Overland

Pacific Marine Environmental Laboratory
Environmental Research Laboratories
Seattle, Washington
April 1980

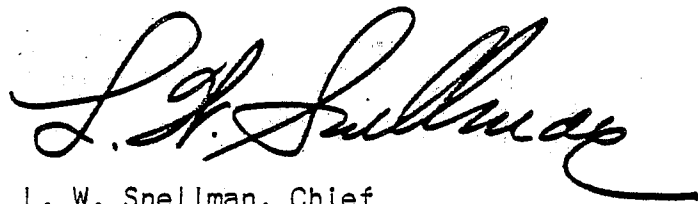
UNITED STATES
DEPARTMENT OF COMMERCE
Philip M. Klutznick,
Secretary

NATIONAL OCEANIC AND
ATMOSPHERIC ADMINISTRATION
Richard A. Frank, Administrator

National Weather
Service
Richard E. Hailgren, Director



This Technical Memorandum has been
reviewed and is approved for
publication by Scientific Services
Division, Western Region.

A handwritten signature in black ink, appearing to read "L. W. Snellman". The signature is written in a cursive style with a long, sweeping tail that extends to the right.

L. W. Snellman, Chief
Scientific Services Division
Western Region Headquarters
Salt Lake City, Utah

CONTENTS

	<u>Page</u>
Tables and Figures	iv
Abstract	1
I. Introduction	1
II. Description of the Models	1
III. Experimental Design	2
IV. Sea-Level Pressure Analyses	3
V. Results	3
VI. Discussion	4
VII. Conclusions	5
VIII. Acknowledgments	5
IX. References	5

TABLES AND FIGURES

		<u>Page</u>
Table 1.	Characteristics of the Various NMC Primitive-Equation Models	7
Table 2.	Difference in Central Pressure Values of the Automated Sea-Level Pressure Analysis and the Hand-Plotted Analysis	7
Table 3.	Means and Standard Deviation of Forecast Central Pressure Error and Location Vector Error Magnitude and Components in kms	8
Table 4.	Median and Hinge Values for Location Vector Error Magnitude	9
Table 5.	Gross Error Table	10
Figure 1.	Sample Sea-Level Pressure Plot	11
Figure 2.	Storm Tracks for the Northeast Pacific, December 1977	12
Figure 3.	Storm Tracks for the Northeast Pacific, 19 January - 28 February 1978	13
Figure 4.	Division of the Northeast Pacific into Three Analysis Regions	14
Figure 5.	Frequency Diagram of the Difference in Central Pressure Values of the NMC Hand-Plotted Sea-Level Pressure Analysis and the Automated Analysis on the LFM and PE Grid	15
Figure 6.	Scatter Plot of Forecast Storm-Center Locations Relative to the Observed Location as the Origin for the LFM-II in December	16
Figure 7.	Scatter Plot of Forecast Storm-Center Locations Relative to the Observed Location as the Origin for the 6LPE in December	17
Figure 8.	Scatter Plot of Forecast Storm-Center Locations Relative to the Observed Location as the Origin for the LFM-II in January - February	18
Figure 9.	Scatter Plot of Forecast Storm-Center Locations Relative to the Observed Location as the Origin for the 7LPE in January - February	19

NMC MODEL PERFORMANCE IN THE NORTHEAST PACIFIC*

James E. Overland
Pacific Marine Environmental Laboratory
Environmental Research Laboratories
NOAA, Seattle, Washington

ABSTRACT. Central pressure and position errors of low centers for 36-hr sea-level pressure forecasts were compared between the LFM-II and 6LPE models for December 1977 and the LFM-II and 7LPE models for 19 January through 28 February 1978. Nine storms provided 41 cases in December and 20 storms provided 66 cases in January through February. During December the LFM-II was superior to the 6LPE in locating rapidly moving storms. The position errors for the LFM-II in December were on the order of 250 km. During February both the LFM-II and the 7LPE had median position errors on the order of 450 km; also, both had a high percentage (25%) of observed-but-not-forecast low centers. The larger errors in February were related to resolution of initial cyclogenesis.

I. INTRODUCTION

The objective of this study is to provide a preliminary evaluation of the effectiveness of the National Meteorological Center (NMC) numerical models in forecasting sea-level pressure in the East Pacific-Gulf of Alaska region during winter. The change of models at NMC provided the opportunity to compare the new Limited Area Fine-Mesh Model (LFM-II), with a resolution of 127 km at 60°N latitude, with the old 6-level hemispheric model (6LPE) and the new 7-level hemispheric model (7LPE). The 7LPE has a grid length of 190.5 km at 60°N, one-half that of the older 6LPE, 381 km. We considered two months of LFM-II forecasts that coincided with the last month of the 6LPE model forecasts and the first month of operational status of the 7LPE model. The evaluation consisted of documenting the errors in central pressure and position of low centers for 36-hr forecasts, a primary interest for coastal weather and ocean-wave forecasting.

II. DESCRIPTION OF THE MODELS

Model characteristics are summarized in Table 1. The original primitive equation model was the hemispheric 6LPE (Shuman and Hovermale, 1968), which became operational June 1966. The LFM became operational September 1971 and covered North America and adjacent waters. The LFM was replaced 31 August 1977, by the new LFM-II (Cooley, 1977a). The LFM-II was intended to incorporate higher spatial resolution, 127.0 km grid length at 60°N versus 190.5 km in the old LFM, without otherwise changing the model's physics. The only major internal change made to the LFM-II was the incorporation of a time-step averaging technique to the pressure gradient terms (Brown and Campana, 1978), which increased the maximum allowable time step. On 18 January 1978, the 6LPE was replaced by the 7LPE. The hemispheric 7LPE has the same mesh length as the old LFM, 190.5 km, and has an additional forecast layer in the stratosphere. The

additional layer has beneficial impact on regional forecasts in the upper layers, but no discernible effect on tropospheric forecasts (Cooley, 1977b).

III. EXPERIMENTAL DESIGN

The data for this study were the NMC grid-point sea-level pressure values for the 0000 and 1200 GMT analyses and 36-hr forecasts from each model for the month of December 1977 and 19 January through 28 February 1978. These grid-point fields were contoured on a polar stereographic projection over the North Pacific using the NCAR-computer graphics routines (Figure 1). Verifying positions and central pressures were determined by the NMC hand-plotted sea-level pressure analyses.

The winter synoptic regime for the Northeast Pacific is characterized by rapidly eastward-moving storms south of 50°N and a tendency for storms to stall and occlude in the Gulf of Alaska and when approaching the west coast of North America. Figures 2 and 3 show the set of tracks of the storms considered in this study for the December and February periods. The December storms moved on generally east-northeast trajectories of the jet stream, stalling near the coast. In February storms tended to curve up along the Canadian coast and move westward into the Gulf of Alaska due to blocking high pressure over Alaska and eastern Canada (Dickson, 1978). The spatial variation in storm movement characteristics led to the division of this region into a rapid movement area, A, and two stall regions, B and C (Figure 4). The contrast between December and February in terms of the larger number of storms, extent of storm generation within the region, and amount of storm recurvature indicated that we were comparing different synoptic climatologies in the two monthly samples.

The basis of forecast accuracy for each model was a comparison between the locations of the forecast low center and the observed low center, and calculation of central pressure differences of these centers for the three areas during the two time periods. Comparisons considered only forecasts showing a reasonable feature for a low center, either an actual closed low or a trough feature, corresponding to an observed closed low or deep trough. Forecasts that missed a surface feature were evaluated separately. Nine storms provided 41 cases in December and 20 storms provided 66 cases in January through February. The majority of December storms were in regions A and C, while most February cases were in region B.

Such a comparison was subject to gross errors. In some cases the continuity of storm systems was in question; in others, the resolution of weak storm systems was in question. Gross errors in selecting cases may have introduced data points that were not members of the population. Medians rather than means were chosen as the appropriate statistic for this study, as they are less subject to the influence of possibly erroneous outlying cases. The dispersion analog to the standard deviation is the h-spread (Tukey, 1977), the numerical difference between the upper and lower quartile values in the data set.

IV. SEA-LEVEL PRESSURE ANALYSES

Three sea-level pressure analyses were available: two objective analyses, corresponding to initializing fields for the two models, and one hand analysis. The finer meshes for the 7LPE and the LFM-II are used only for finite difference computation; the analysis fields and the forecast output fields are on the scale of their parent models, 381 and 190.5 km at 60°N.

Table 2 and Figure 5 compare the two machine analyses with the hand analysis for central pressure. There was approximately a 2-mb positive bias in the LFM-II analysis and a 3-mb bias in the 6LPE and 7LPE analysis. The h-spread was 4 mb for the LFM-II in December and 3 mb for all other cases. The analysis bias of the PE models relative to the LFM-II may be due to the use of a coarse mesh for interpolation and smoothing. The hemispheric models also use a spectral type analysis scheme (Flattery, 1970), which is known to have a slight bias of not making sharp troughs and strong lows deep enough; whereas, the LFM-II uses local interpolation (Cressman, 1959).

V. RESULTS

The separation of the forecast low center from the verifying observed low center for the three areas is shown for December for the LFM-II in Figure 6 and for the 6LPE in Figure 7. The x/y coordinates of the forecast position were recorded relative to the observed position as the origin. If one model failed to identify a case predicted by the other model, the forecast for the second model was indicated by an (x). These cases were subsequently excluded from the analysis. Figures 6 and 7 also show a histogram of central pressure errors. Table 3 lists mean and standard deviation of central pressure algebraic error, and the mean magnitude and standard deviation of the components of the vector error (x,y) in kms. Table 4 lists the median and upper and lower hinge values for the magnitude of the location vector error.

In region A for December, the LFM-II was superior to the 6LPE in locating fast-moving storms with median error distances of 250 km (LFM-II) and 574 km (6LPE). This is apparent from the scatter plots, Figures 6 and 7. The 6LPE had a fairly Gaussian distribution of forecasts about the verifying position; whereas, the LFM-II results consisted of a cluster of forecasts a short distance southwest of the origin with two major outlying points to the northeast. Central pressure errors were comparable for both models. Shifting to region B, 10 of the 13 cases considered a single storm that stalled in the central Gulf of Alaska. Both models showed small errors in position. Central pressures, however, were consistently underforecast, i.e., higher than observed. In two cases both models underforecast on the order of 10 - 15 mb. In region C the LFM-II had a slight advantage over the 6LPE in central pressure and similar errors in location. Both models, but particularly the 6LPE, tended to forecast south of the observed position.

During the period 19 January - 28 February, the performance of the LFM-II contrasted with that of December (Figure 8). In area A the mean and median position error and central pressure errors were greater than during the December period. The LFM-II tended to place storms to the north of their observed locations. As most storms were on a north-northeast trajectory, this implied speeds of propagation faster than those observed. The new 7LPE

(Figure 9) showed results similar to the LFM-II in region A. The 7LPE also had a position bias to the north, although not as great as that of the LFM-II. The position error diagrams for both models showed Gaussian-type scatter in contrast to those of the LFM-II for December. In the northern section, area B, the 7LPE was superior to the LFM-II. Neither model showed position error bias. In February, region C contained only five samples. The 7LPE had large position-error statistics based upon two outlying points in a small sample.

We now consider the category of missed features. A missed feature is any forecast that does not exhibit a strong similarity in cyclonic curvature of the isobars corresponding to a closed low or significant trough feature on the observed map, or any forecast that has a low center which is not observed. Table 5 lists observed-but-not-forecast low centers and forecast-but-not-observed centers. Storms in December consisted of several major lows with long trajectories that were consistently forecast by the LFM-II. In February, out of 66 forecasts, the LFM-II missed features on 18 and the 7LPE missed on 15. Recourse to the daily maps indicated that many of these cases occurred during the early development of lows within the analysis region. However, one 989-mb low center was missed for four consecutive 7LPE forecasts despite its continued presence in the initialization fields. The last column of Figure 5 indicates the cases in which only one model forecast showed a significant feature. The low numbers indicate that both the LFM-II and the 7LPE tended to miss features on the same forecasts. Five of the eight cases which were forecast by the 7LPE but not the LFM-II were in the northwest quadrant of the region near the edge of the LFM-II grid. In several of the cases where the LFM-II provided the forecast, the 7LPE tended to be either slow to develop or too fast to weaken a storm.

VI. DISCUSSION

This study provides a comparison of truncation errors of three different mesh sizes: 127 km, 190.5 km, and 381 km, for short-term forecasts over the North Pacific. As the December cases clearly indicate, there is an improvement in position error and ability to forecast observed features in the fine mesh LFM-II compared to the coarse-mesh 6LPE. Brown (1975) showed a similar conclusion after comparing the old LFM with the 6LPE for 30 forecasts of winter east-coast storms. However, our analysis showed the 7LPE in February performed at a comparable level to the LFM-II, suggesting the existence of a threshold value of mesh length for estimating storm motion in the North Pacific.

Shuman (1978) showed continued improvement in forecasting the location of surface low-pressure centers over the eastern United States for mesh lengths as small as 60 km. Shuman showed selected days of strong storm development that warrant a finer mesh. Indeed many of the storms in our observed-but-not-forecast category were tied to initial development, an implication consistent with the earlier studies of Leary (1971) and Brown (1974).

Although all three models in this study have ostensibly the same model physics, damping due to effective model viscosity and overt smoothing is reduced with smaller grid size. The LFM-II in December showed many good forecasts with a few extreme outlying cases. The average northward displacement of lows in region A in February also showed a tendency for the model to

move storms faster than observed. Given the data gaps in upper-air observations over the Pacific as compared to the coverage over the continental United States, one can speculate that misplaced features would develop more readily with a finer mesh model. Thus, while a fine mesh may give a superior forecast for a selected case, a mesh length of 100 - 200 km is a good compromise length for current NMC models when performance evaluation is median position statistics.

During February many storms passed near the Aleutian Island Chain near the edge of the LFM-II model domain. This led to observed-but-not-forecast errors for the LFM-II in February and, probably, larger position and central-pressure errors as well.

VII. CONCLUSIONS

A comparison was made between the LFM-II and 6LPE and 7LPE models based upon 107 36-hr forecasts of sea-level pressure from December 1977 and from 19 January through 28 February 1978. The magnitude of forecast errors depended on the location, speed, and age of the particular storm. The LFM-II was superior to the 6LPE in locating rapid movement of storms. The LFM-II median position error was 250 km in region A for December. The LFM-II and the new 7LPE performed in a similar fashion during February. Both had median position errors in region A on the order of 450 km and a high percentage of observed-but-not-forecast storm systems. Even within regional groupings, the set of storms formed a heterogeneous collection of central pressures, forward speeds, and directions. From this set of data no clear bias for position errors could be determined.

VIII. ACKNOWLEDGMENTS

I wish to thank W. Gemmill for his assistance in obtaining the NMC data set and L. W. Snellman for his thoughtful review. This paper is a contribution to the Pacific Marine Environmental Laboratory Marine Services Program. J. Vimont and S. Ghan assisted in data tabulation.

IX. REFERENCES

- Brown, H. E., 1974: Performance Characteristics of NMC's Numerical Models and Services of the Basic Weather Forecast Branch. Advanced Prediction Techniques Course, National Weather Service, National Oceanic and Atmospheric Administration (NOAA), U. S. Dept. of Commerce (DOC), 59 pp.
- Brown, H. E., 1975: Comparison of the Position and Central Pressure Errors of East Coast Lows on 36-Hour PE and LFM Prognoses. NMC Technical Attachment 75-4, 6 pp.
- Brown, J. A. and K. A. Campana, 1978: An Economical Time-Differencing System for Numerical Weather Prediction. Mon. Wea. Rev. 106, 1125-1136.
- Cooley, D. S., 1977a: High Resolution LFM (LFM-II). Technical Procedures Bulletin No. 206, National Weather Service, NOAA, DOC, 6 pp.

- Cooley, D. S., 1977b: The 7LPE Model. Technical Procedures Bulletin No. 218, National Weather Service, NOAA, DOC, 14 pp.
- Cressman, G. P., 1959: An Operational Objective Analysis System. Mon. Wea. Rev. 87, 367-374.
- Dickson, R. R., 1978: Weather and Circulation of February 1978. Mon. Wea. Rev. 106, 746-751.
- Flattery, T. W., 1970: Spectral Models for Global Analysis and Forecasting. Proceedings, Sixth AWS Technical Exchange Conference, AWS Tech. Report 242, Scott AFB, Ill., 42-54.
- Leary, C., 1971: Systematic Errors in Operational National Meteorological Center Primitive-Equation Surface Prognoses. Mon. Wea. Rev. 99, 409-413.
- Shuman, F. G., 1978: Numerical Weather Prediction. Bull. Amer. Meteor. Soc. 59, 5-17.
- Shuman, F. G. and J. B. Hovermale, 1968: An Operational Six-layer Primitive Equation Model. Journal of Applied Meteorology 7, 525-547.
- Tukey, J. W., 1977: Exploratory Data Analysis. Addison-Wesley, Phillipines, 506 pp.

TABLE 1

CHARACTERISTICS OF THE VARIOUS NMC PRIMITIVE EQUATION MODELS

MODEL	AREA	NO. OF LEVELS	GRID SIZE @60 NORTH	DATES
6LPE	N. Hemisphere	6	381. km	June 66 - Jan 78
LFM	N. America	6	190.5	Sept 71 - Aug 77
LFM-II	N. America	6	127.0	Sept 77 -
7LPE	N. Hemisphere	7	190.5	Feb 78 -

TABLE 2

DIFFERENCE IN CENTRAL PRESSURE VALUES OF THE AUTOMATED SEA LEVEL PRESSURE ANALYSIS AND THE HAND PLOTTED ANALYSIS (MACHINE CP) - (HAND CP) IN MB

	MODEL	CASES	MEDIAN	MEAN	SD
Dec.	LFM-II	37	1.	1.28	3.51
	6LPE	37	3.	3.11	3.31
Jan.-	LFM-II	39	2.	2.03	3.46
Feb.	7LPE	39	3.	3.56	3.60

TABLE 3

MEANS AND STANDARD DEVIATION OF FORECAST CENTRAL PRESSURE ERROR AND LOCATION VECTOR ERROR
MAGNITUDE AND COMPONENTS IN KMS. CENTRAL PRESSURE ERRORS ARE OBSERVED MINUS FORECAST IN MBS.

	Type	Region	Cases	CP DIF		DIST		X(east)		Y(north)		$\sqrt{x^2 + y^2}$
				Mean	SD	Mean	SD	Mean	S_x	Mean	S_y	
D E C	LFM-II	A	16	-3.1	5.1	350	276	63	285	-85	339	106
	LFM-II	B	13	-9.2	6.8	252	150	-28	241	89	152	93
	LFM-II	C	8	0.5	6.8	367	102	159	250	-70	282	174
	6LPE	A	16	-2.1	5.0	507	220	-96	361	-106	395	143
	6LPE	B	13	-8.0	7.8	263	137	-48	204	39	193	61
	6LPE	C	8	-4.1	7.6	410	239	-48	258	-363	237	367
19 J A N F E B	LFM-II	A	11	-5.9	7.8	504	244	28	395	287	317	289
	LFM-II	B	23	-6.7	7.8	437	278	-61	415	-15	361	63
	LFM-II	C	5	-8.0	7.8	474	287	278	436	-30	258	280
	7LPE	A	11	-7.7	5.2	436	276	26	276	158	423	159
	7LPE	B	23	-5.6	6.6	358	309	-87	228	95	278	128
	7LPE	C	5	-5.2	3.6	471	228	-78	463	-82	526	113

TABLE 4

MEDIAN AND HINGE VALUES FOR LOCATION VECTOR ERROR MAGNITUDE

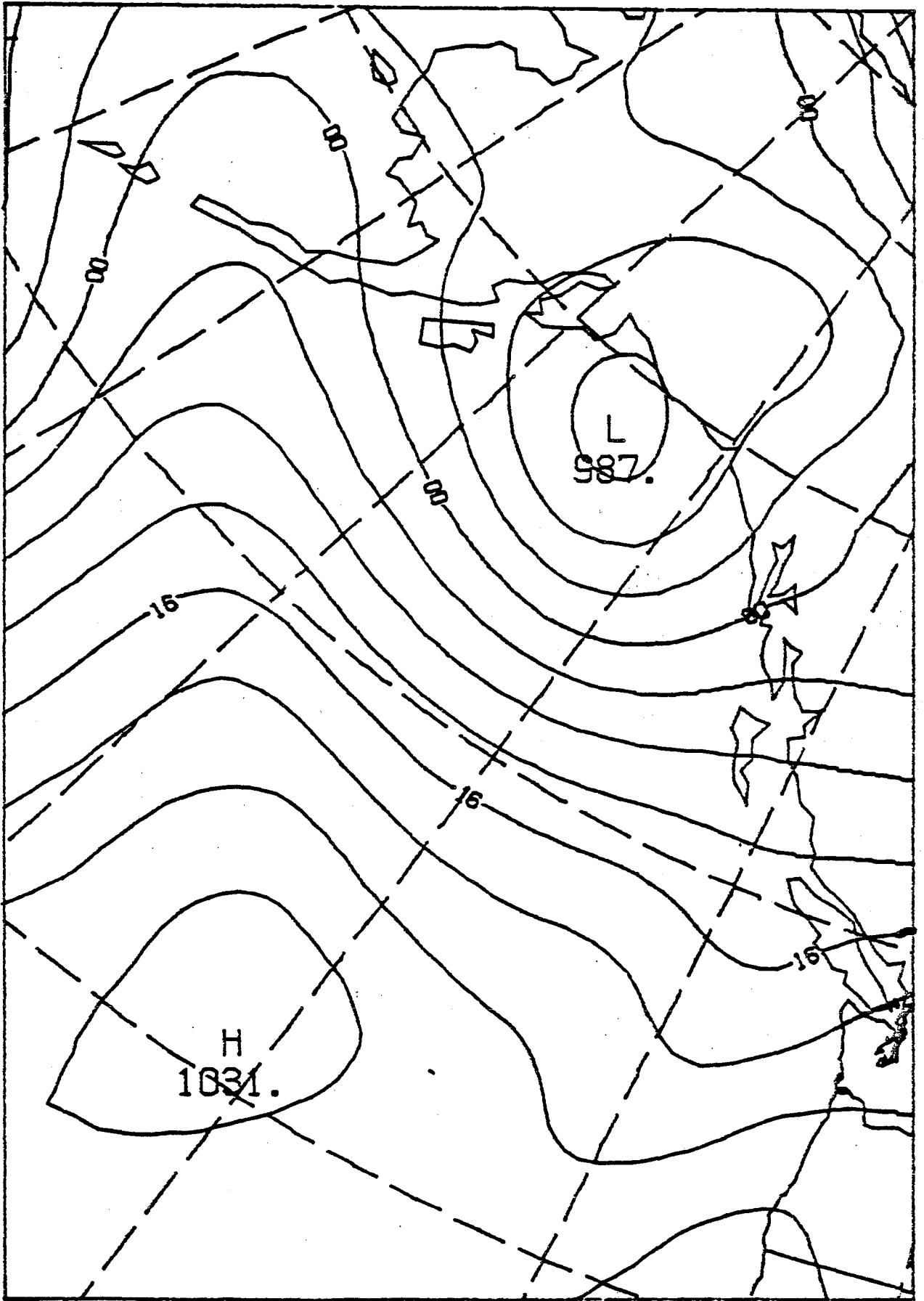
Type	Region	Cases	Hinge	DIST Median	Hinge	Hinge	X Median	Hinge	Hinge	Y Median	Hinge	
D E C E M B E R	LFM-II	A	16	148	250	389	-130	-37	130	-259	-93	-56
	LFM-II	B	13	111	259	371	-130	-56	56	-19	74	204
	LFM-II	C	8	287	417	426	-37	222	398	-278	-139	74
	6LPE	A	16	306	574	695	-398	-167	-28	-389	-195	222
	6LPE	B	13	185	241	278	-241	0	93	-93	-37	148
	6LPE	C	8	259	408	426	-148	9	158	-426	-380	-241
19 Jan- Feb.	LFM-II	A	11	352	445	621	-250	37	176	65	408	500
	LFM-II	B	23	241	371	621	-232	19	269	-46	0	139
	LFM-II	C	5	315	500	741	74	334	649	-222	-56	37
	7LPE	A	11	241	463	612	-158	74	195	-148	37	537
	7LPE	B	23	167	259	445	-195	-93	65	-56	37	185
	7LPE	C	5	259	537	649	-278	-204	-111	-259	-56	130

TABLE 5

GROSS ERROR TABLE

Type	Observed, Not Forecast	Forecast, Not Observed	Single Forecasts
Dec LFM-II	0	2	4
6LPE	4	1	0
Jan LFM-II	18	5	5
Feb 7LPE	15	4	8

36 HR FCST SLP



00Z 23 JAN 1978

Figure 1. Sample Sea-Level Pressure Plot.

december 1977

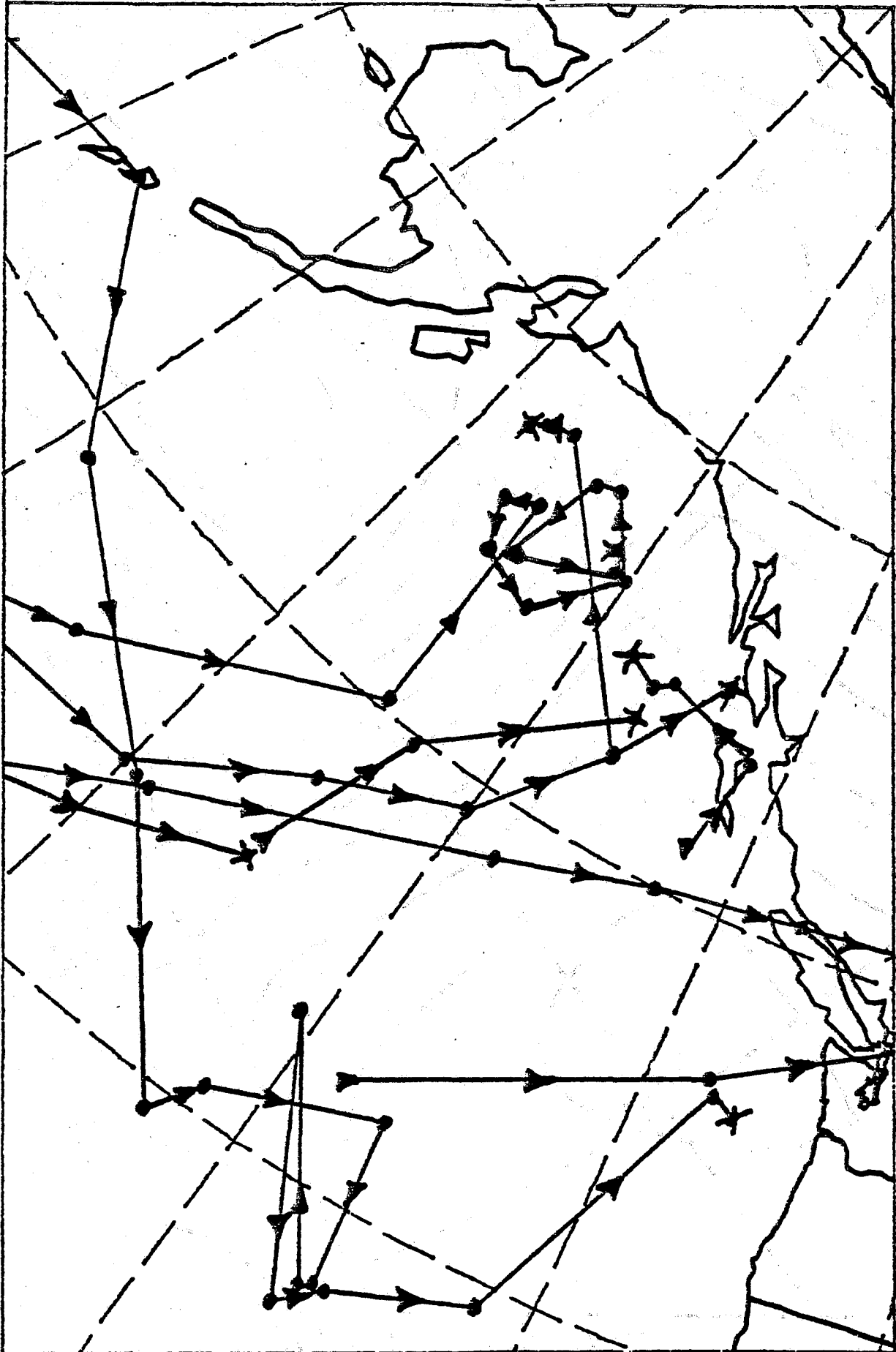


Figure 2. Storm Tracks for the Northeast Pacific, December 1977.

19 january - february 1978

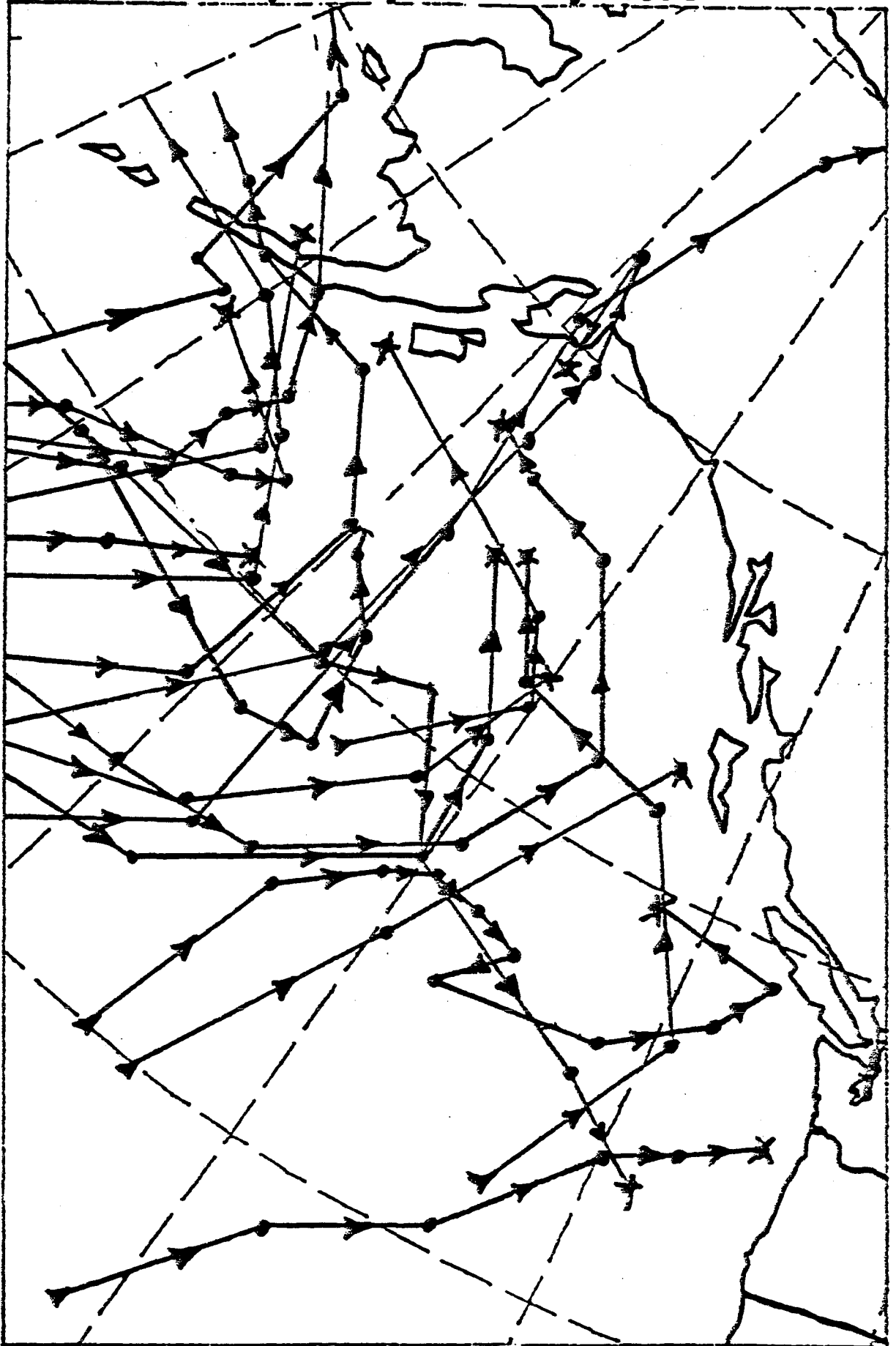


Figure 3. Storm Tracks for the Northeast Pacific, 19 January - 28 February 1978.

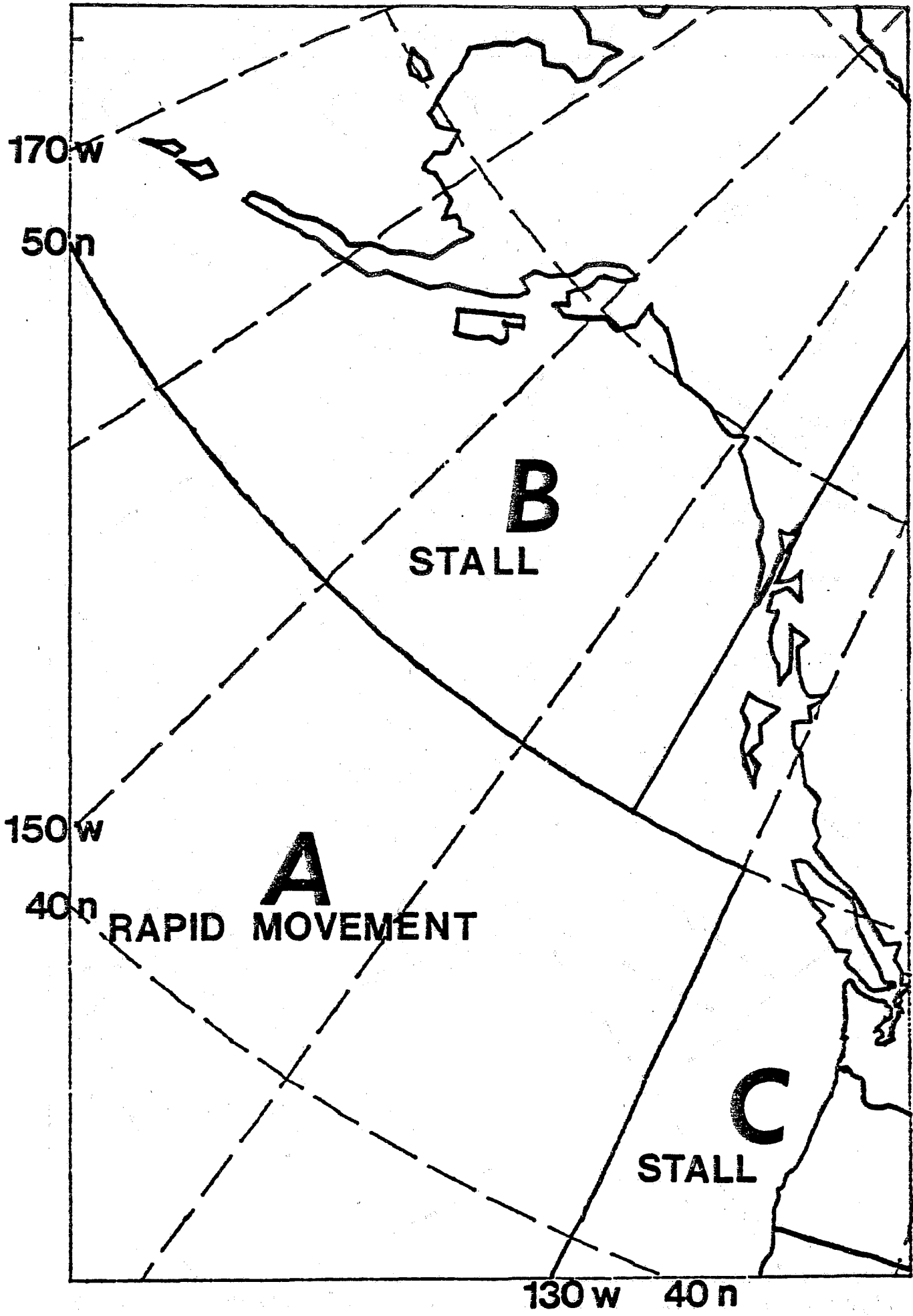


Figure 4. Division of the Northeast Pacific into Three Analysis Regions.

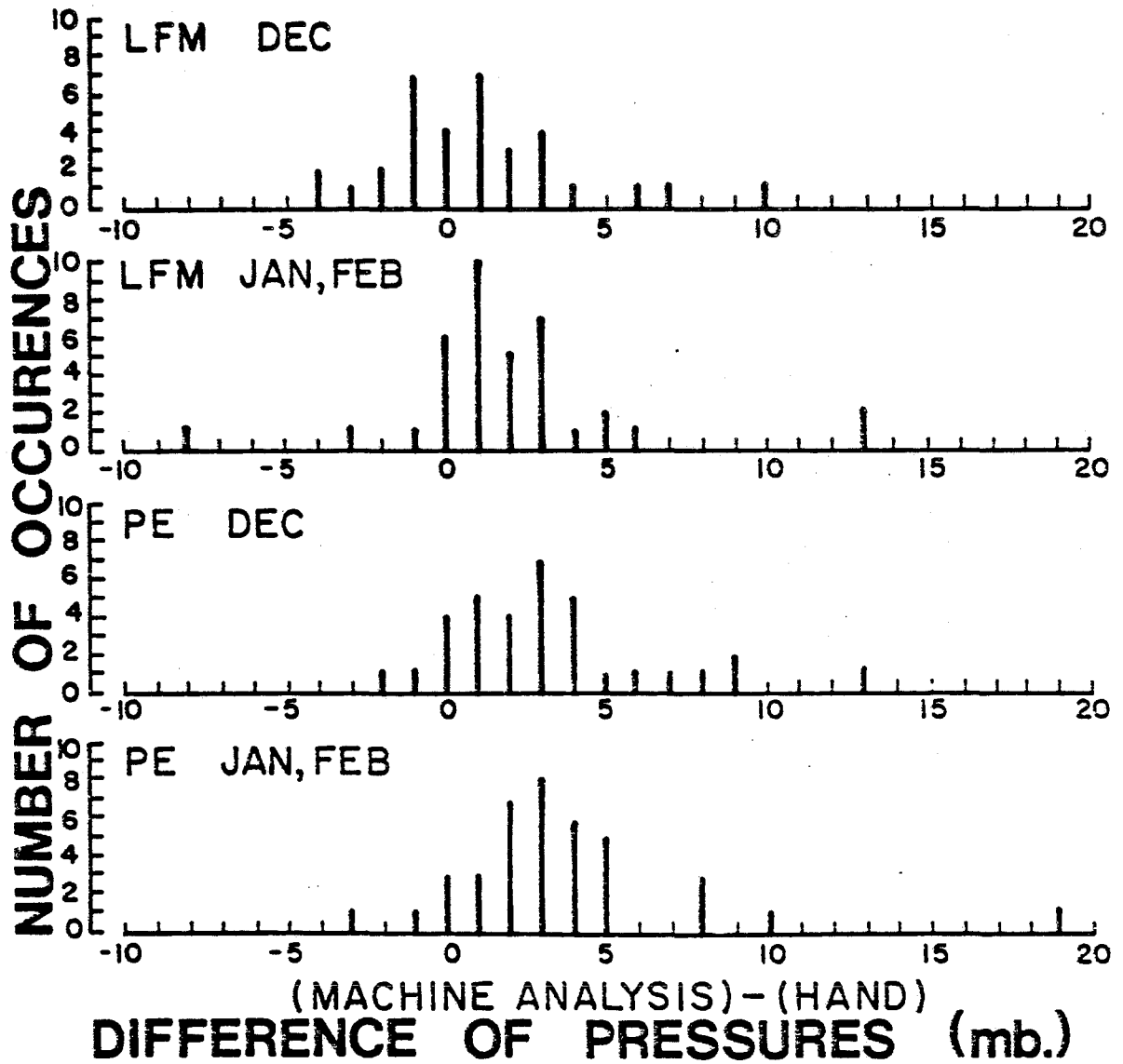


Figure 5. Frequency diagram of the difference in central pressure values of the NMC hand-plotted sea-level pressure analysis and the automated analysis on the LFM and PE grid.

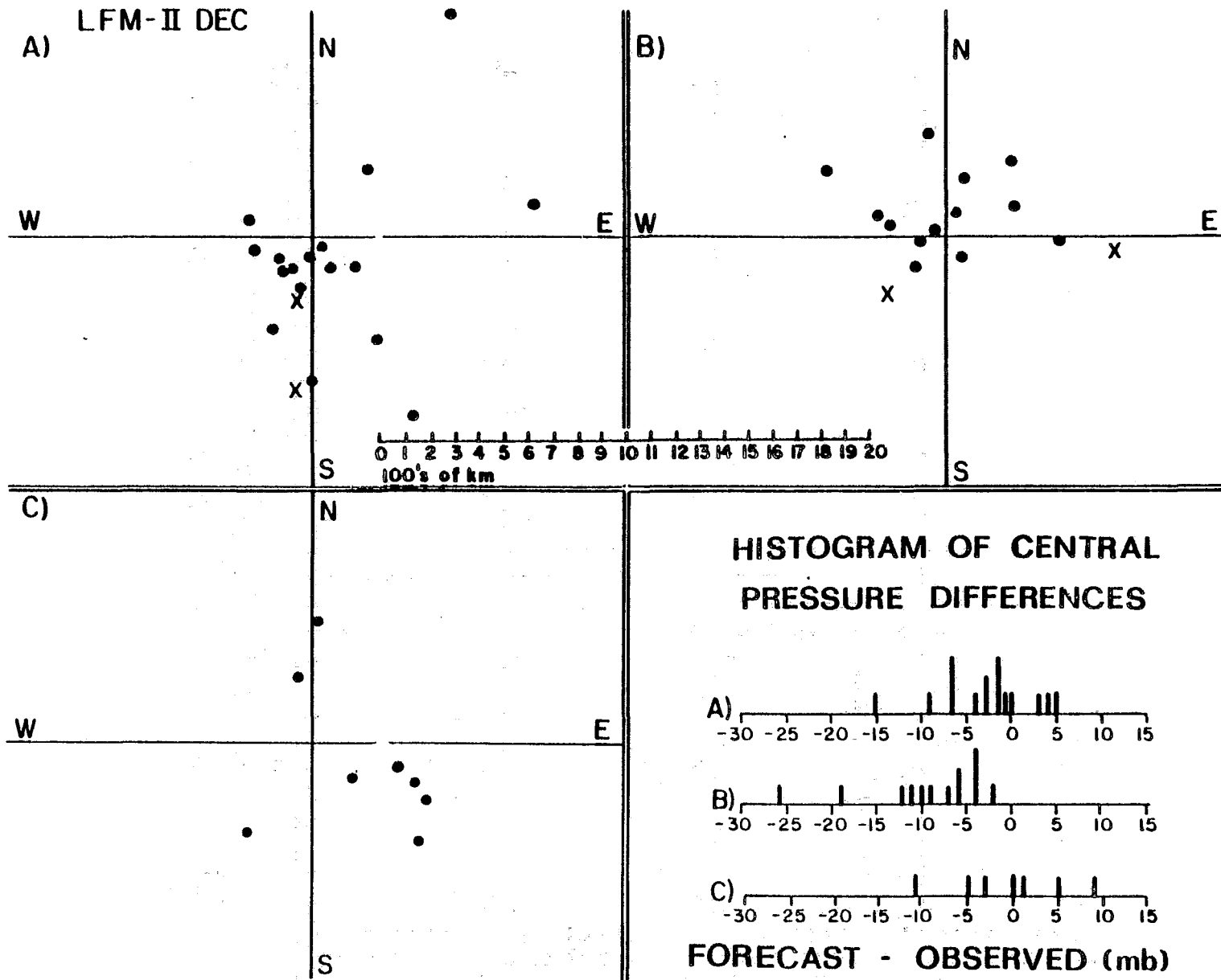


Figure 6. Scatter plot of forecast storm-center locations relative to the observed location as the origin for the LFM-II in December. Lower left corner shows the frequency distribution of forecast central pressures minus observed central pressures.

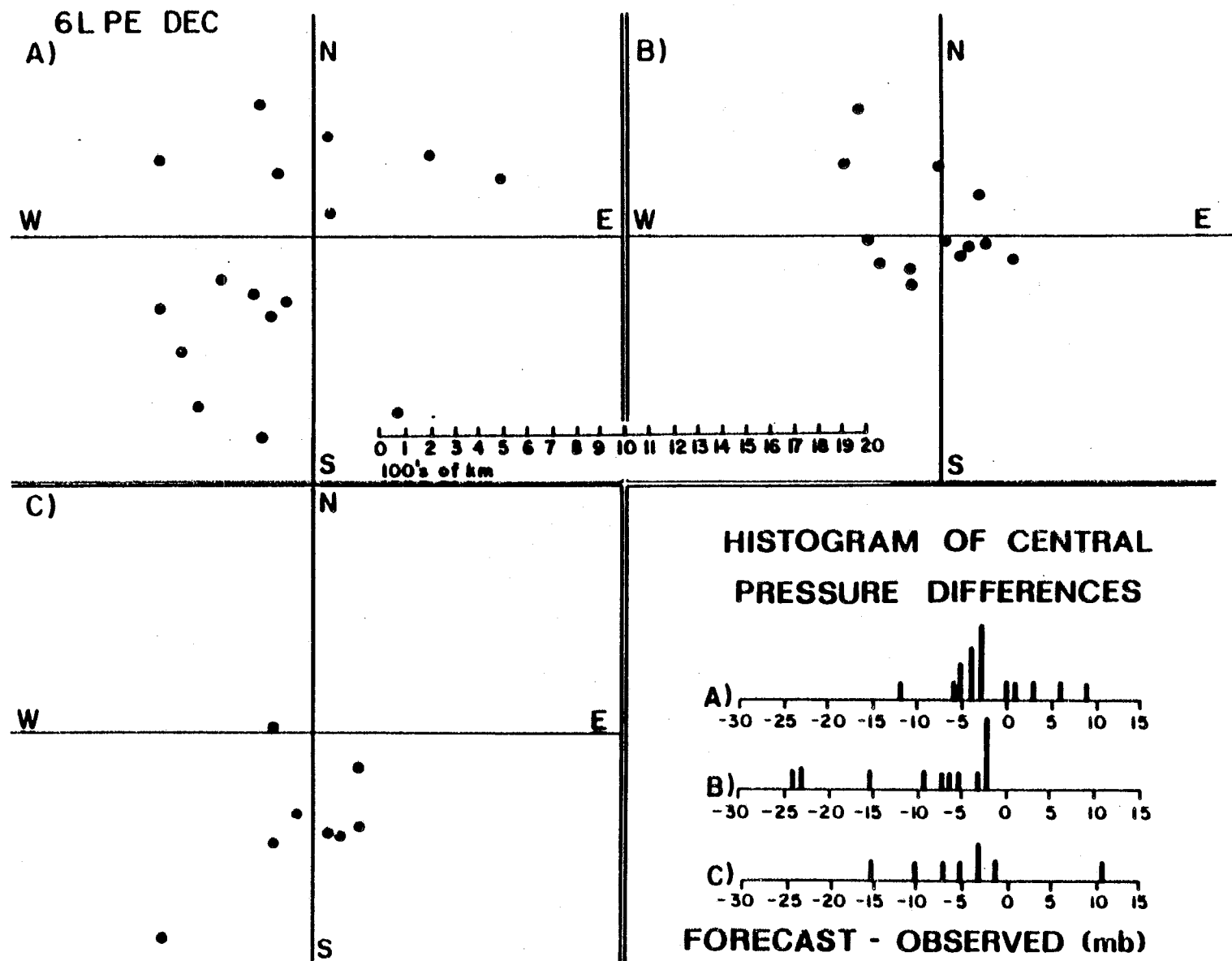


Figure 7. Scatter plot of forecast storm-center locations relative to the observed location as the origin for the 6LPE in December. Lower left corner shows the frequency distribution of forecast central pressures minus observed central pressures.

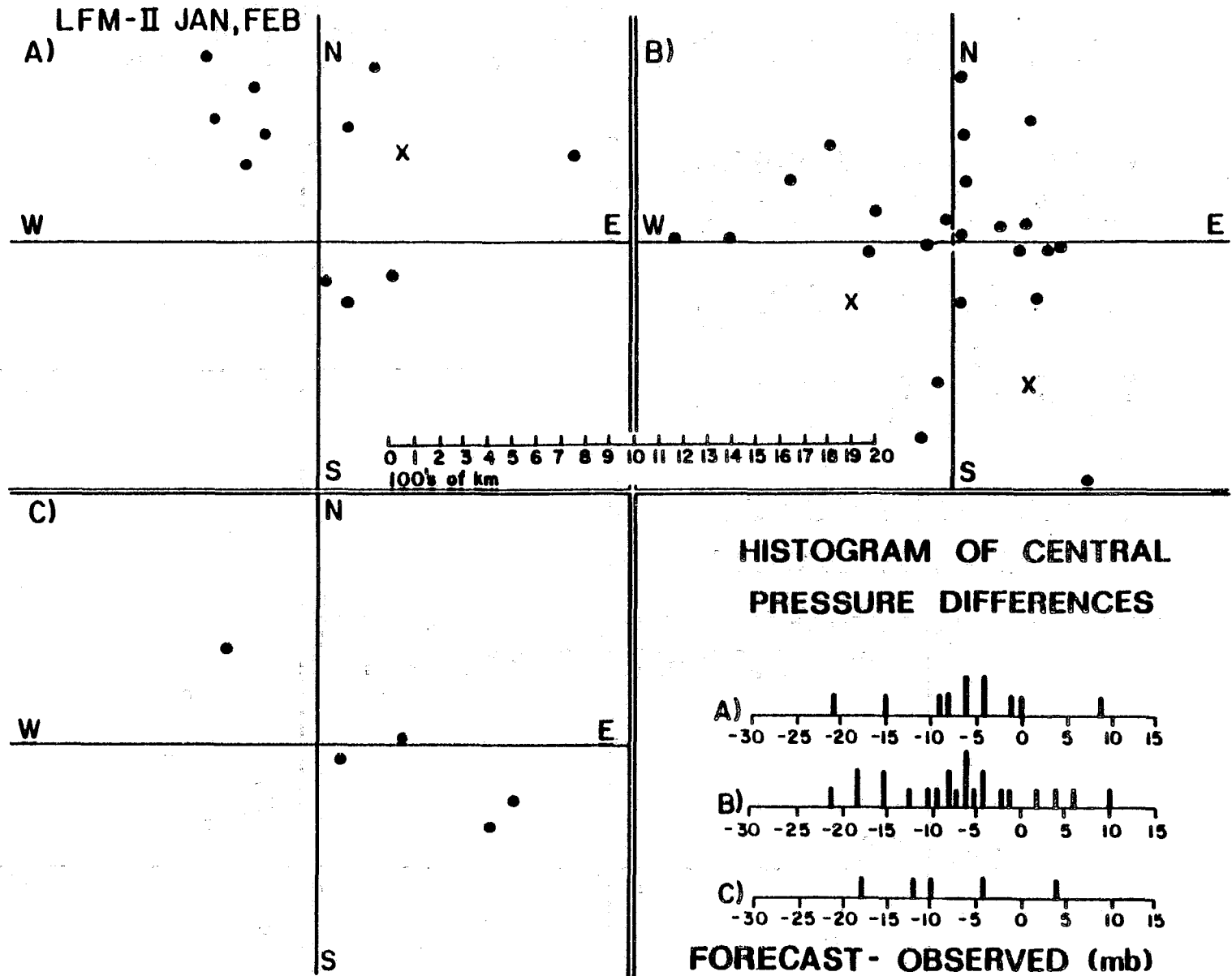


Figure 8. Scatter plot of forecast storm-center locations relative to the observed location as the origin for the LFM-II in January - February. Lower left corner shows the frequency distribution of forecast central pressures minus observed central pressures.

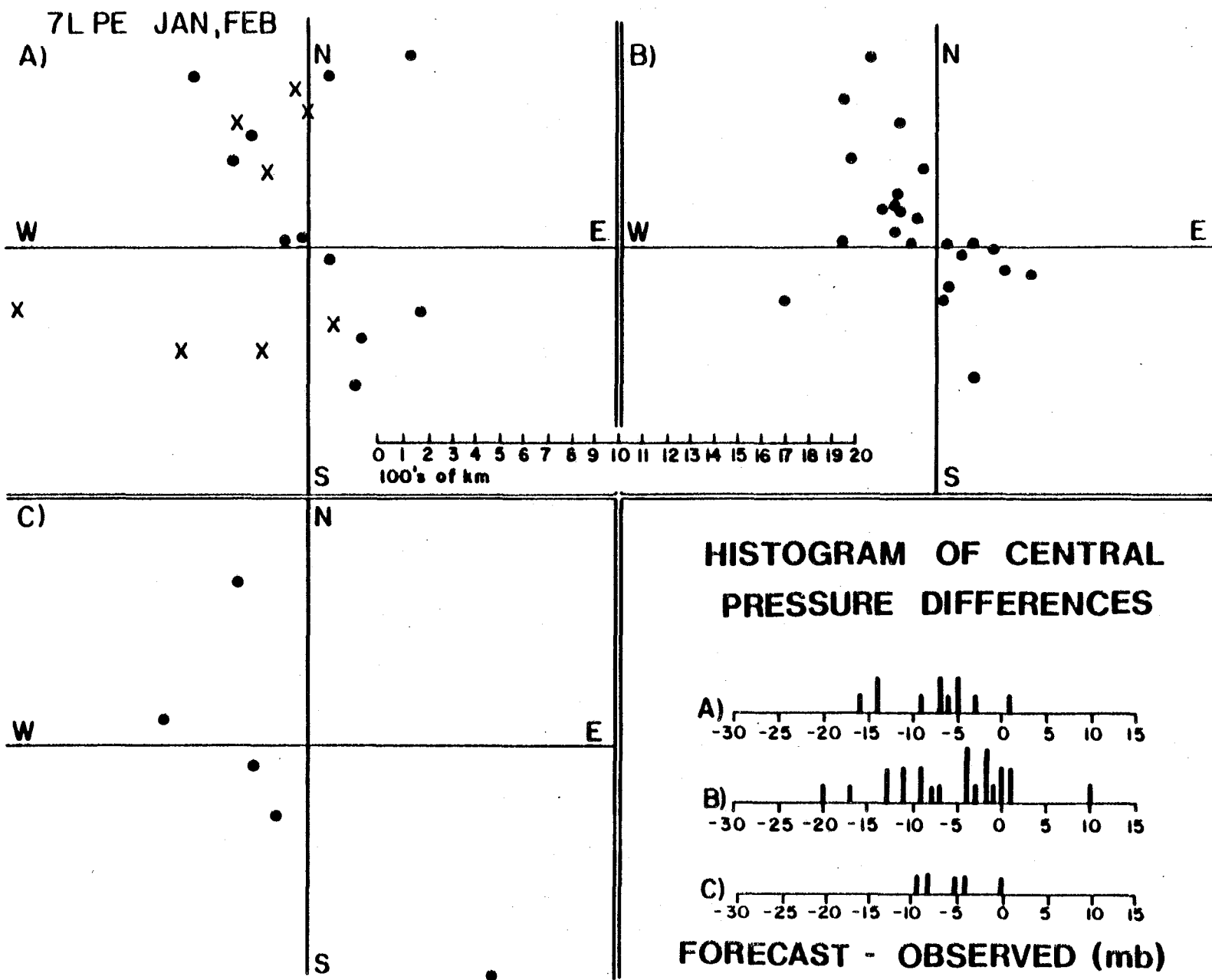


Figure 9. Scatter plot of forecast storm-center locations relative to the observed location as the origin for the 7LPE in January - February. Lower left corner shows the frequency distribution of forecast central pressures minus observed central pressures.

- 92 Smoke Management in the Willamette Valley. Earl M. Bates, May 1974. (COM-74-11277/AS)
- 93 An Operational Evaluation of 500-mb Type Regression Equations. Alexander E. MacDonald, June 1974. (COM-74-11407/AS)
- 94 Conditional Probability of Visibility Less than One-Half Mile in Radiation Fog at Fresno, California. John D. Thomas, August 1974. (COM-74-11555/AS)
- 96 Map Type Precipitation Probabilities for the Western Region. Glenn E. Rasch and Alexander E. MacDonald, February 1975. (COM-75-10428/AS)
- 97 Eastern Pacific Cut-off Low of April 21-23, 1974. William J. Alder and George R. Miller, January 1976. (PB-250-711/AS)
- 98 Study on a Significant Precipitation Episode in Western United States. Ira S. Brenner, April 1976. (COM-75-10719/AS)
- 99 A Study of Flash Flood Susceptibility--A Basin in Southern Arizona. Gerald Williams, August 1975. (COM-75-11360/AS)
- 102 A Set of Rules for Forecasting Temperatures in Napa and Sonoma Counties. Wesley L. Truff, October 1975. (PB-246-902/AS)
- 103 Application of the National Weather Service Flash-Flood Program in the Western Region. Gerald Williams, January 1976. (PB-253-053/AS)
- 104 Objective Aids for Forecasting Minimum Temperatures at Reno, Nevada, During the Summer Months. Christopher D. Hill, January 1976. (PB-252-366/AS)
- 105 Forecasting the Mono Wind. Charles P. Ruscha, Jr., February 1976. (PB-254-650)
- 106 Use of MOS Forecast Parameters in Temperature Forecasting. John C. Plankinton, Jr., March 1976. (PB-254-649)
- 107 Map Types as Aids in Using MOS PoPs in Western United States. Ira S. Brenner, August 1976. (PB-259-594)
- 108 Other Kinds of Wind Shear. Christopher D. Hill, August 1976. (PB-260-437/AS)
- 109 Forecasting North Winds in the Upper Sacramento Valley and Adjoining Forests. Christopher E. Fontana, Sept. 1976. (PB-273-677/AS)
- 110 Cool Inflow as a Weakening Influence on Eastern Pacific Tropical Cyclones. William J. Denny, November 1976. (PB-264-655/AS)
- 112 The MAN/MOS Program. Alexander E. MacDonald, February 1977. (PB-265-941/AS)
- 113 Winter Season Minimum Temperature Formula for Bakersfield, California, Using Multiple Regression. Michael J. Card, February 1977. (PB-273-694/AS)
- 114 Tropical Cyclone Kathleen. James R. Fors, February 1977. (PB-273-676/AS)
- 116 A Study of Wind Gusts on Lake Mead. Bradley Colman, April 1977. (PB-268-847)
- 117 The Relative Frequency of Cumulonimbus Clouds at the Nevada Test Site as a Function of K-value. R. F. Quiring, April 1977. (PB-272-831)
- 118 Moisture Distribution Modification by Upward Vertical Motion. Ira S. Brenner, April 1977. (PB-268-740)
- 119 Relative Frequency of Occurrence of Warm Season Echo Activity as a Function of Stability Indices Computed from the Yucca Flat, Nevada, Rawlinsenda. Barryl Randerson, June 1977. (PB-271-290/AS)
- 121 Climatological Prediction of Cumulonimbus Clouds in the Vicinity of the Yucca Flat Weather Station. R. F. Quiring, June 1977. (PB-271-704/AS)
- 122 A Method for Transforming Temperature Distribution to Normality. Morris S. Webb, Jr., June 1977. (PB-271-742/AS)
- 124 Statistical Guidance for Prediction of Eastern North Pacific Tropical Cyclone Motion - Part I. Charles J. Neumann and Preston W. Leftwich, August 1977. (PB-272-661)
- 125 Statistical Guidance on the Prediction of Eastern North Pacific Tropical Cyclone Motion - Part II. Preston W. Leftwich and Charles J. Neumann, August 1977. (PB-273-153/AS)
- 127 Development of a Probability Equation for Winter-Type Precipitation Patterns in Great Falls, Montana. Kenneth B. Mielko, February 1978. (PB-281-387/AS)
- 128 Hand Calculator Program to Compute Parcel Thermal Dynamics. Dan Gudgeal, April 1978. (PB-285-080/AS)
- 129 Fire Whirls. David W. Coens, May 1978. (PB-285-386/AS)
- 130 Flash-Flood Procedures. Ralph G. Hatch and Gerald Williams, May 1978. (PB-285-014/AS)
- 131 Automated Fire-Weather Forecasts. Mark A. Moliner and David E. Olson, September 1978. (PB-289-916/AS)
- 132 Estimates of the Effects of Terrain Blocking on the Los Angeles WSR-74C Weather Radar. R. G. Peppers, R. Y. Lee, and B. M. Finko, October 1978. (PB289767/AS)
- 133 Spectral Techniques in Ocean Wave Forecasting. John A. Jannuzzi, October 1978. (PB291317/AS)
- 134 Solar Radiation. John A. Jannuzzi, November 1978. (PB291193/AS)
- 135 Application of a Spectrum Analyzer in Forecasting Ocean Swell in Southern California Coastal Waters. Lawrence P. Kierulff, January 1979. (PB292716/AS)
- 136 Basic Hydrologic Principles. Thomas L. Dietrich, January 1979. (PB292247/AS)
- 137 LFM 24-Hour Prediction of Eastern Pacific Cyclones Refined by Satellite Images. John R. Zimmerman and Charles P. Ruscha, Jr., January 1979. (PB294324/AS)
- 138 A Simple Analysis/Diagnosis System for Real Time Evaluation of Vertical Motion. Scott Hoffick and James R. Fors, February 1979. (PB294216/AS)
- 139 Aids for Forecasting Minimum Temperature in the Wenatchee Frost District. Robert S. Robinson, April 1979. (PB293339/AS)
- 140 Influence of Cloudiness on Summertime Temperatures in the Eastern Washington Fire Weather District. James Halscom, April 1979. (PB293674/AS)
- 141 Comparison of LFM and MFM Precipitation Guidance for Nevada During Doreen. Christopher Hill, April 1979. (PB293613/AS)
- 142 The Usefulness of Data from Mountain-top Fire Lookout Stations in Determining Atmospheric Stability. Jonathan W. Corvay, April 1979. (PB293899/AS)
- 143 The Depth of the Marine Layer at San Diego as Related to Subsequent Cool Season Precipitation Episodes in Arizona. Ira S. Brenner, May 1979. (PB293817/AS)
- 144 Arizona Cool Season Climatological Surface Wind and Pressure Gradient Study. Ira S. Brenner, May 1979. (PB293900/AS)
- 145 On the Use of Solar Radiation and Temperature Models to Estimate the Snap Bean Maturity Date in the Willamette Valley. Earl M. Bates, August 1979. (PB30165112)
- 146 The BART Experiment. Morris S. Webb, October 1979. (PB30165112)
- 147 Occurrence and Distribution of Flash Floods in the Western Region. Thomas L. Dietrich, December 1979.
- 148 A Real-Time Radar Interface for AFOS. Mark Mathewson, January 1980.
- 149 Misinterpretations of Precipitation Probability Forecasts. Allan H. Murphy, Sarah Lichtenstein, Baruch Fishbein, and Robert L. Winkler, February 1980.
- 150 Annual Data and Verification Tabulation - Eastern and Central North Pacific Tropical Storms and Hurricanes 1979. Eric S. Gunther and Staff, EPAC, April 1980.

NOAA SCIENTIFIC AND TECHNICAL PUBLICATIONS

NOAA, the *National Oceanic and Atmospheric Administration*, was established as part of the Department of Commerce on October 3, 1970. The mission responsibilities of NOAA are to monitor and predict the state of the solid Earth, the oceans and their living resources, the atmosphere, and the space environment of the Earth, and to assess the socioeconomic impact of natural and technological changes in the environment.

The six Major Line Components of NOAA regularly produce various types of scientific and technical information in the following kinds of publications:

PROFESSIONAL PAPERS—Important definitive research results, major techniques, and special investigations.

TECHNICAL REPORTS—Journal quality with extensive details, mathematical developments, or data listings.

TECHNICAL MEMORANDUMS—Reports of preliminary, partial, or negative research or technology results, interim instructions, and the like.

CONTRACT AND GRANT REPORTS—Reports prepared by contractors or grantees under NOAA sponsorship.

TECHNICAL SERVICE PUBLICATIONS—These are publications containing data, observations, instructions, etc. A partial listing: Data serials; Prediction and outlook periodicals; Technical manuals, training papers, planning reports, and information serials; and Miscellaneous technical publications.

ATLAS—Analyzed data generally presented in the form of maps showing distribution of rainfall, chemical and physical conditions of oceans and atmosphere, distribution of fishes and marine mammals, ionospheric conditions, etc.



Information on availability of NOAA publications can be obtained from:

**ENVIRONMENTAL SCIENCE INFORMATION CENTER
ENVIRONMENTAL DATA SERVICE
NATIONAL OCEANIC AND ATMOSPHERIC ADMINISTRATION
U.S. DEPARTMENT OF COMMERCE**

**3300 Whitehaven Street, N.W.
Washington, D.C. 20235**